Supplemental Material

Structure-function analysis of the OB and latch domains of *Chlorella* virus DNA ligase

Poulami Samai and Stewart Shuman

From the Molecular Biology Program, Sloan-Kettering Institute, New York, NY 10065

Supplemental Experimental Procedures

Supplemental Figures S1, S2, S3 and S4

Supplemental Table S1

Experimental Procedures

ChVLig purity and concentration. The total protein concentrations of the recombinant WT and mutant ChVLig preparations were determined by using the Bio-Rad dye reagent with bovine serum albumin as a standard. Aliquots (nominally 6 μg as measured by dye-binding) of the ChVLig preparations were analyzed by SDS-PAGE (12% polyacrylamide) and polypeptides were visualized by staining with Coomassie blue dye (Fig. S1). The gels were then scanned with Kodak Image Pro 4000R instrument. Image Gauge software was then used to obtain a densitometric profile of each ChVLig electropherogram as follows: (i) full-length scans of individual lanes were collected through the centers of the lanes using a band width of ~60% of the total lane width; (ii) the intensity profile for each lane was baseline corrected; (iii) the areas under the peaks corresponding to ChVLig and any contaminating peptides were determined. The percent purity of each preparation was then calculated as the ratio of the ChVLig peak to the sum off all peak intensities in the lane. The results are as follows: WT (85%), F190A (84%), S235A (86%), T249A (82%), K274A (81%), K274Q (82%), K274R (81%), F276A-M278A (78%), K281A-C283A (77%), S235A-K281A-C283A (86%), R285A (92%), R285K (91%), R285Q (94%), F286A (87%), F286L (91%), V288A (93%), V288I (93%), V288T (93%), N214A (91%), N214D (91%), N214L (90%), N214Q (88%), F215A (86%), F215L (85%), Y217A (82%), Y217F (86%), Y217L (86%), Y217S (83%), S218A-R220A (82%), S221A-T222A-H223A (90%). The WT purity value was then used to determine the amount of WT ChVLig protein corresponding to the integrated area under the ChVLig polypeptide peak. The amounts of the mutant ChVLig protein were calculated by scaling the integrated areas under the mutant ChVLig polypeptide peaks to that of WT ChVLig.

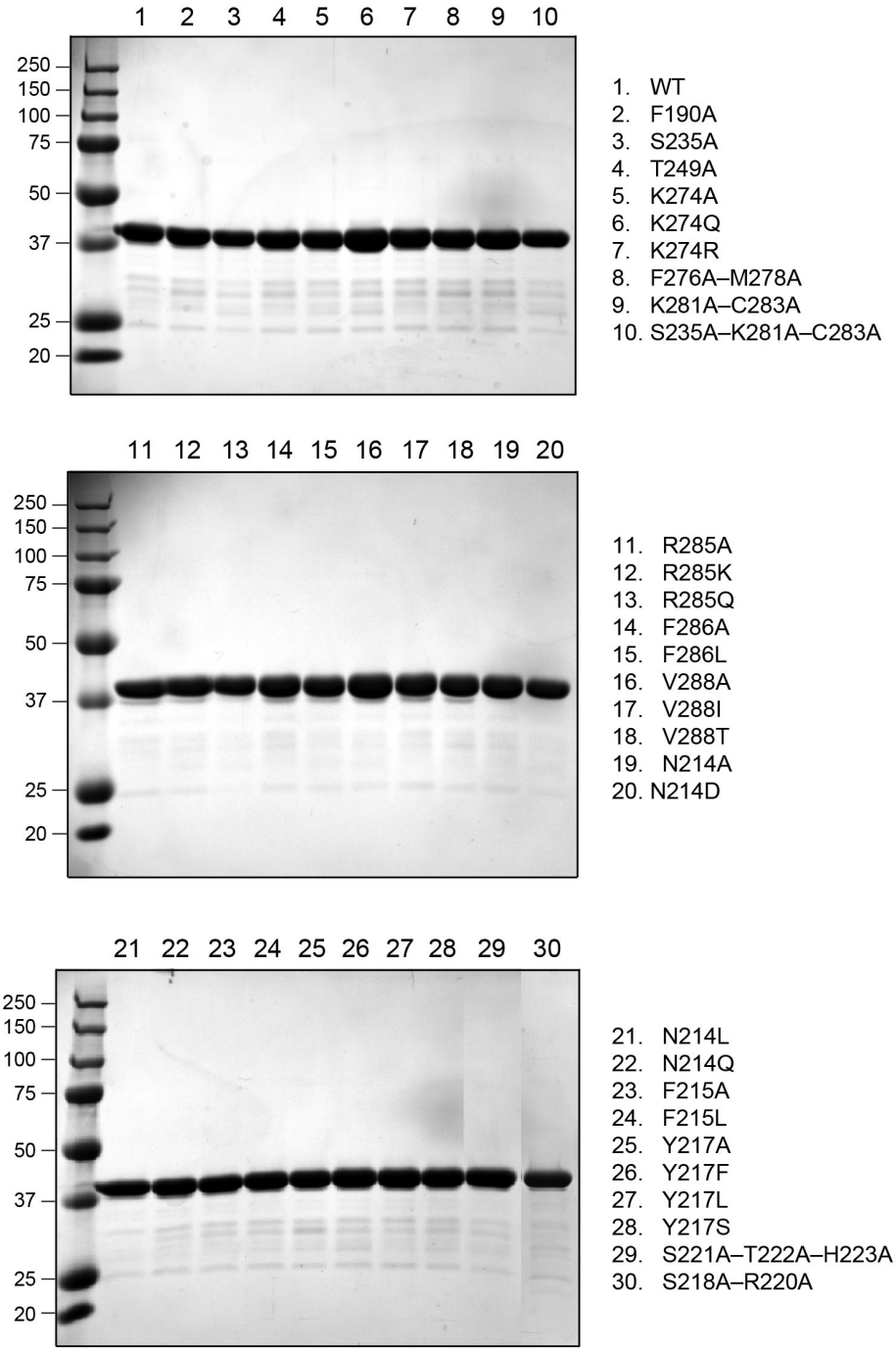

Figure S1. **ChVLig proteins**. Aliquots (6 µg) of the phosphocellulose fractions of wild-type (WT) ChVLig and the indicated ChVLig mutants were analyzed by SDS-PAGE. The Coomassie blue-stained gels are shown. The positions and sizes (kDa) of marker polypeptides are indicated on the *left*.

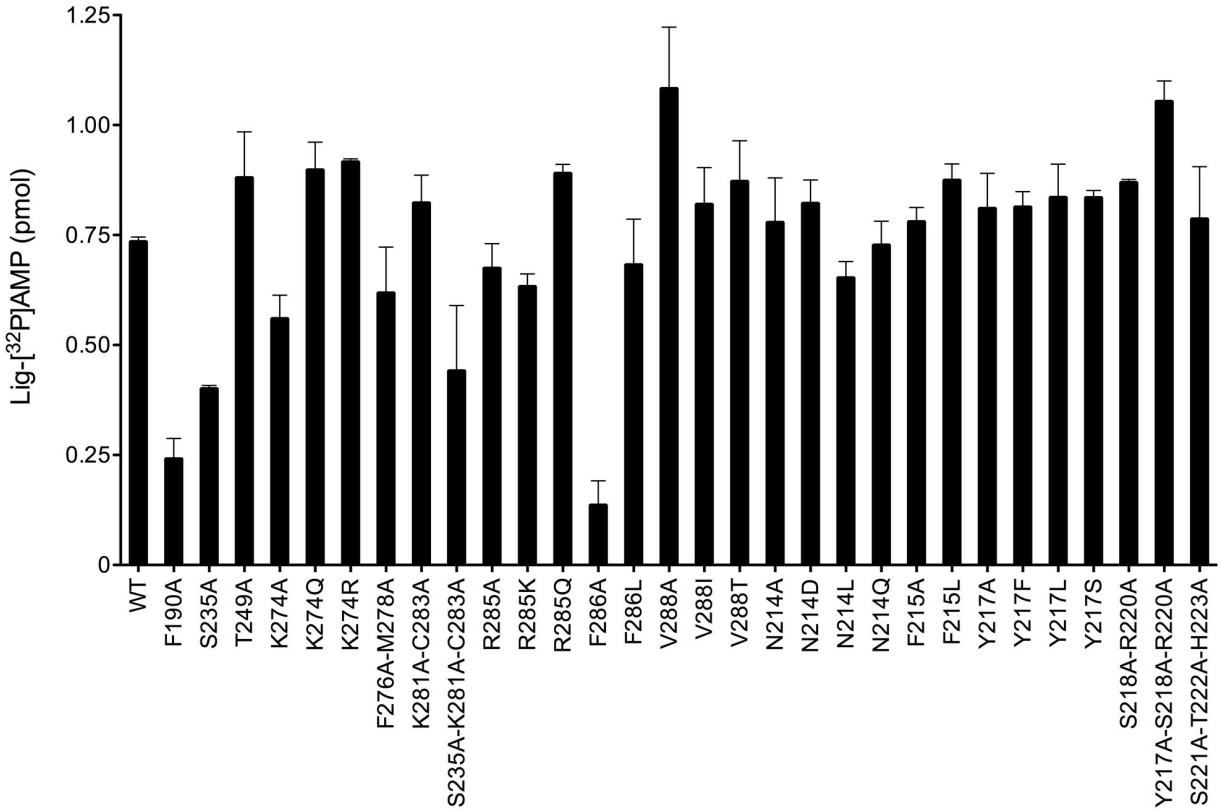

Figure S2. **Ligase adenylylation *in vitro***. Reaction mixtures (20 µl) containing 50 mM Tris-HCl (pH 7.5), 5 mM DTT, 5 mM $MgCl_2$, 100 µM [α-^{32}P]ATP, and 2 pmol of wild-type or mutant ChVLig were incubated at 37°C for 10 min. The reactions were quenched by adding SDS to 1% final concentration. The reaction products were analyzed by SDS-PAGE. The ChVLig–[^{32}P]AMP adduct was visualized by autoradiography of the dried gels and quantified by scanning the gels with a Fujix BAS2500 imager. Each datum is the average of three separate adenylylation experiments ±SEM.

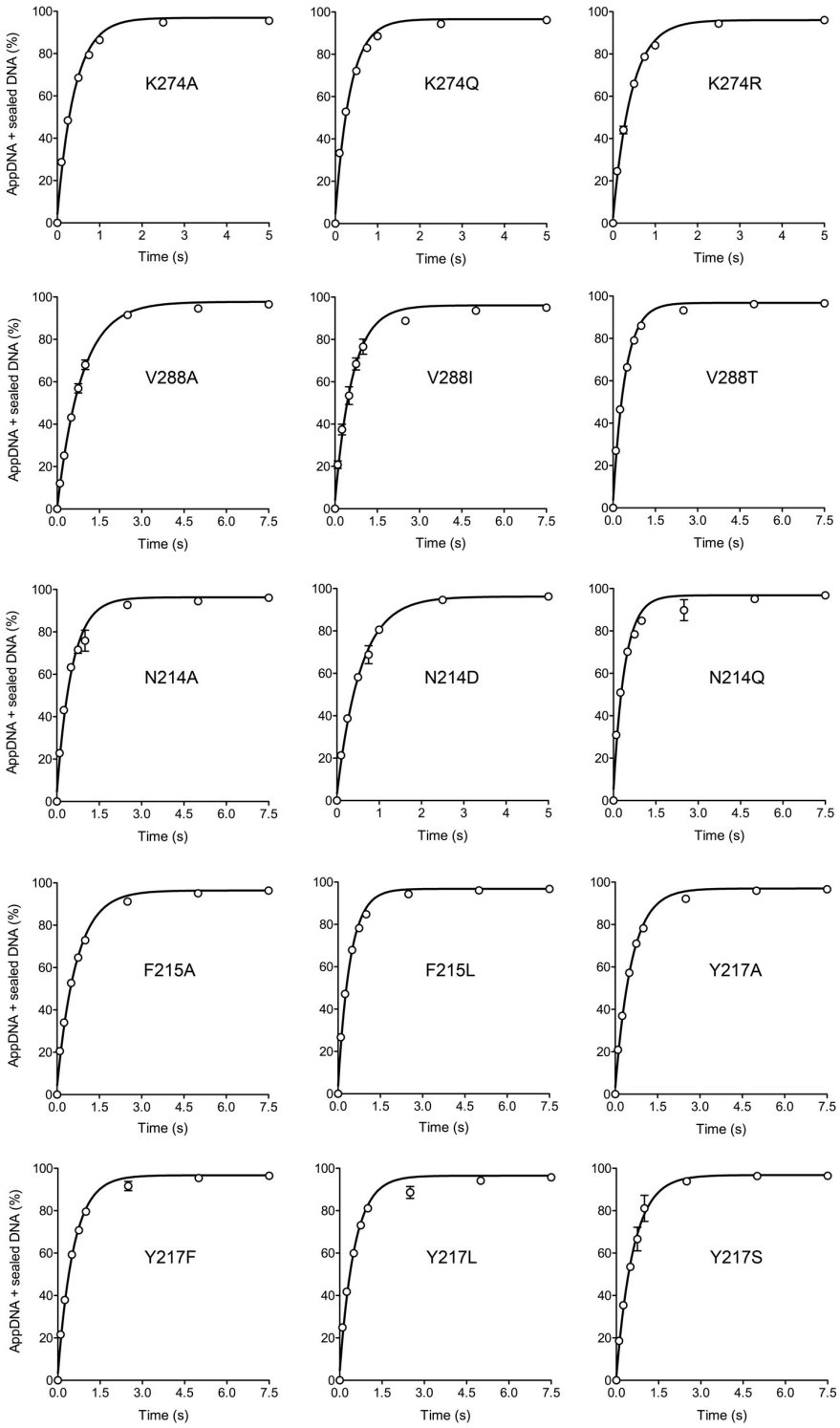

Figure S3. **Kinetics of single-turnover DNA adenylylation and nick sealing by pre-adenylylated ChVLig-AMP**. The rate of step 2 catalysis (DNA adenylylation) was gauged by plotting the sum of AppDNA plus sealed DNA as function of reaction time for the mutant ChVLig preparations specified. Each datum in the graphs is the average of three separate kinetic experiments ±SEM. Nonlinear regression curve fitting of the data to a single exponential was performed in Prism.

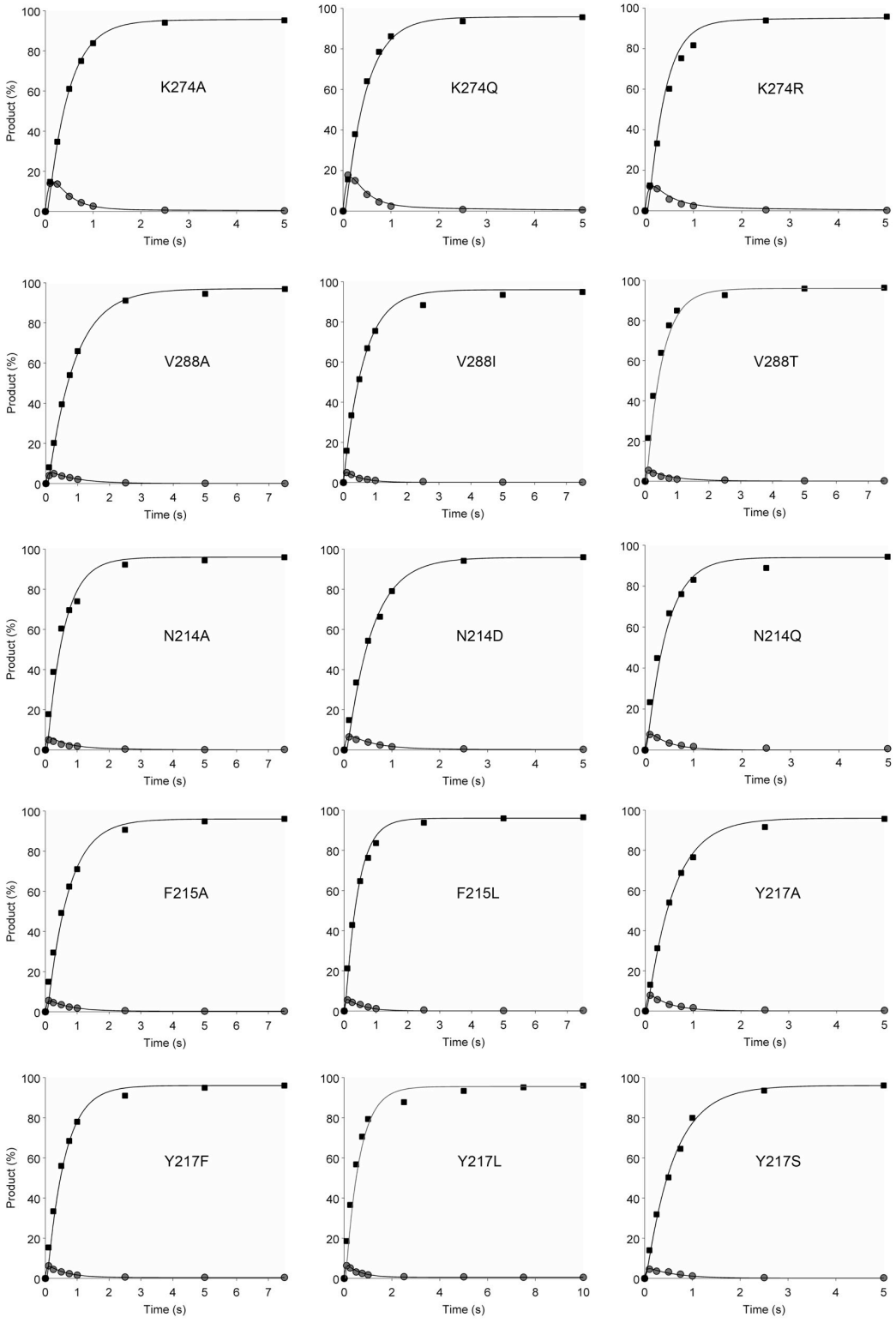

Figure S4. **Kinetics of single-turnover nick sealing**. The distributions of 18-mer AppDNA intermediate (gray circles) and sealed 36-mer DNA (black squares) during single-turnover nick sealing by the indicated ChVLig-AMP proteins are plotted as a function of reaction time. Each datum in the graphs is the average of three separate kinetic experiments. The curve fits to the kinetic scheme in Fig. 4 are shown.

Table S1

Distinctive mutational effects on DNA adenylylation and phosphodiester synthesis

ChVLig	Step 2 rate constant (s^{-1})[a]	Step 3 rate constant (s^{-1})[b]	k_{out} (s^{-1})	k_{in}(s^{-1})
WT	2.3 ± 0.09	24.1 ± 1.69	0.18 ± 0.02	0.15 ± 0.05
K274A	2.69 ± 0.12	11.5 ± 0.38	0.15 ± 0.06	0.14 ± 0.01
K274Q	3.05 ± 0.13	11 ± 0.61	0.25 ± 0.09	0.3 ± 0.05
K274R	2.4 ± 0.06	14 ± 0.8	0.25 ± 0.01	0.23 ± 0.08
R285A	0.06 ± 0.001	0.2 ± 0.01	<0.01	<0.01
R285K	0.08 ± 0.001	0.46 ± 0.01	0.006 ± 0.001	0.007 ± 0.001
R285Q	0.06 ± 0.001	0.24 ± 0.01	0.008 ± 0.001	0.006 ± 0.001
F286A	0.11 ± 0.01	2.01 ± 0.35	<0.01	<0.01
F286L	0.74 ± 0.08	17.5 ± 2	0.16 ± 0.06	0.1 ± 0.05
V288A	1.19 ± 0.02	17.7 ± 0.58	0.11 ± 0.09	4.75 ± 2.75
V288I	1.95 ± 0.17	31.5 ± 2	<0.01	<0.01
V288T	2.07 ± 0.2	30.8 ± 2.18	0.5 ± 0.17	1 ± 0.3
N214A	1.87 ± 0.07	23.5 ± 1.45	0.2 ± 0.05	0.6 ± 0.16
N214D	1.85 ± 0.1	21.8 ± 0.83	0.04 ± 0.01	<0.01
N214Q	2.44 ± 0.1	22.7 ± 1.38	<0.01	<0.01
F215A	1.46 ± 0.14	21.1 ± 1.5	0.06 ± 0.04	<0.01
F215L	2.48 ± 0.16	27.4 ± 1.26	<0.01	<0.01
Y217A	1.8 ± 0.06	22.5 ± 1.87	<0.01	0.01 ± 0.05
Y217F	1.88 ± 0.09	23.3 ± 2.27	0.09 ± 0.03	<0.01
Y217L	1.73 ± 0.25	21.5 ± 2.32	0.11 ± 0.03	<0.01
Y217S	1.7 ± 0.07	28.3 ± 1.65	0.07 ± 0.05	<0.01

The experimental kinetic profiles for the AppDNA intermediate and sealed DNA end-product (Fig. 4 and S4) were modeled in MATLAB to the kinetic scheme depicted in Fig. 4. The four component rate constants derived thereby are tabulated above ± the 95% confidence intervals.